J. Synchrotron Rad. (1998). **5**, 679–681

Position of exit X-rays from rotated-inclined double-crystal monochromators

Yasuharu Kashihara,[a]* Hiroshi Yamazaki,[a] Kenji Tamasaku[b] and Tetsuya Ishikawa[c]

[a]Japan Synchrotron Radiation Research Institute, Kamigouri, Ako-gun, Hyogo 678-12, Japan, [b]Microwave Laboratory, RIKEN, Kamigouri, Ako-gun, Hyogo 678-12, Japan, and [c]JAERI-RIKEN SPring-8 Project Team, Kamigouri, Ako-gun, Hyogo 678-12, Japan. E-mail: kashi@haru01.spring8.or.jp

(*Received 4 August 1997; accepted 3 November 1997*)

The rotated-inclined double-crystal monochromator (RIDCM) has been adopted to reduce the heat load from third-generation undulator radiation. The position of the exit X-rays from RIDCM has been calculated as a function of X-ray energy on the basis of diffraction theory including refraction effects. The results show that the positions of the exit X-rays vary over a wide range due to asymmetric reflection. Methods of fixing the exit position in RIDCM are also discussed.

Keywords: double-crystal monochromators; rotated-inclined double-crystal monochromators; exit X-rays; undulator monochromators; SPring-8.

1. Introduction

The European Synchrotron Radiation Facility (ESRF), the Advanced Photon Source (APS) and SPring-8 are third-generation synchrotron facilities operated at 6, 7 and 8 GeV, respectively, in which X-ray undulators will be the main light sources. The heat-load problem with undulator monochromators arises from the power density rather than the total power. In order to overcome the heat problem, several methods, including geometrical reduction of the power density on the first crystal of a double-crystal monochromator, have been adopted. For example, the inclined double-crystal monochromator (IDCM) (Blasdell *et al.*, 1994; Hrdy, 1992; Khounsary, 1992; Lee *et al.*, 1992; Lee & Mills, 1994; Macrander *et al.*, 1992) with liquid-Ga cooling and the rotated-inclined double-crystal monochromator (RIDCM) (Uruga *et al.*, 1995) with pin-post water cooling have been developed at APS and SPring-8, respectively.

The vertical and horizontal positions of the exit X-rays from IDCM and RIDCM can be easily fixed for various X-ray energies, if the diffraction of X-rays follows the kinematical diffraction theory. Actual X-rays refract at the entrance and exit surfaces of a crystal so that the exit X-rays from the monochromator deviate from the position calculated using the kinematical diffraction theory. We therefore examine the exit X-ray position by using diffraction theory including refraction effects and discuss ways to fix the exit X-ray position.

2. Optical arrangements of RIDCM

The optical arrangement of RIDCM is illustrated in Fig. 1. $\mathbf{K}_O$ and $\mathbf{K}_H$ are the wave vectors of the incident and reflected X-rays on the first crystal, respectively. $\mathbf{K}_{H'}$ is the wavevector of the exit X-ray from the second crystal. γ_O and γ_H (or $\gamma_{O'}$ and $\gamma_{H'}$) are the polar angles between the incident and reflected X-rays and the normal to the crystal surface $\mathbf{n}$ (or $\mathbf{n}'$), respectively, and are defined as shown in Fig. 1. The inclination angle between the normal $\mathbf{n}$ (or $\mathbf{n}'$) and the active reciprocal lattice vector $\mathbf{H}$ (or $\mathbf{H}'$) of the crystal is denoted as β. The RIDCM is set so that the surfaces of two crystals are parallel to each other and $\mathbf{H}'$ is parallel to $\mathbf{H}$. Then the exit X-ray $\mathbf{K}_{H'}$ from the second crystal is always parallel to the incident X-ray $\mathbf{K}_O$.

Let us consider an orthogonal coordinate system, O_1-XYZ, fixed in an experimental hall. We take the Z axis in the direction of the incident X-ray $\mathbf{K}_O$, the Y axis in the vertical plane and the X axis in the horizontal plane. Let the intersection of the incident X-ray $\mathbf{K}_O$ and the surface of the first crystal be the origin O_1 of the coordinate system. The exit X-ray $\mathbf{K}_{H'}$ from the double-crystal monochromator intersects the image screen perpendicular to the Z axis at the point (X, Y).

To realize the fixed exit we put the second crystal at O_2 with the vector $\overline{O_1O_2}$ in O_1-XYZ written as

$$\overline{O_1O_2} = (0, g, g/\tan 2\theta_B), \tag{1}$$

where g is a nominal offset value and θ_B is the kinematic Bragg angle. In the kinematical diffraction theory the point (X, Y) on the image screen is represented by (0, g) since $\mathbf{H}$ and $\mathbf{H}'$ are usually in the Y-Z plane; the real image point, however, is different from the point (0, g) because of refraction.

3. Diffraction condition

To examine the diffraction condition of X-rays on RIDCM we define an orthogonal coordinate system, O_1-$X'Y'Z'$, fixed on the first crystal surface as shown in Fig. 2. We take the Z' axis in the $\mathbf{n}$ direction and the Y' axis perpendicular to the plane which is spanned by the vectors $\mathbf{n}$ and $\mathbf{H}$. The X' axis is perpendicular to both the Y' and Z' axes. Let an azimuthal angle of the incident X-ray wavevector $\mathbf{K}_O$ around the Z' axis be ψ_O with respect to the X' axis. Similarly, let the azimuthal angle for the diffracted X-ray wavevector $\mathbf{K}_H$ be ψ_H.

In the kinematical X-ray diffraction theory, the incident X-ray can be reflected from the crystal when the incident angles, polar angle γ_{KO} and azimuthal angle ψ_{KO} satisfy

$$\sin\gamma_{KO}\cos\psi_{KO}\sin\beta + \cos\gamma_{KO}\cos\beta = H/2K, \tag{2}$$

where H and K are magnitudes of the reciprocal lattice vector $\mathbf{H}$ and the incident X-ray wavevector $\mathbf{K}_O$, respectively. The diffracted X-ray calculated in the kinematical X-ray diffraction theory have exit angles, polar angle γ_{KH} and azimuthal angle ψ_{KH} satisfying

$$\cos\gamma_{KH} = -\cos\gamma_{KO} + (H/K)\cos\beta, \tag{3}$$

$$\sin\psi_{KH} = -\sin\psi_{KO}\sin\gamma_{KO}/\sin\gamma_{KH}, \tag{4}$$

$$\cos\psi_{KH} = [-\cos\psi_{KO}\sin\gamma_{KO} + (H/K)\sin\beta]/\sin\gamma_{KH}. \tag{5}$$

However, the X-ray actually refracts through the entrance and exit surfaces of a crystal and so, for diffraction, γ_O, ψ_O, γ_H and ψ_H must be different from those calculated in the kinematical diffraction theory. If their deviations are represented by $\Delta\gamma_O$, $\Delta\psi_O$, $\Delta\gamma_H$ and $\Delta\psi_H$, then the real angles

can be written

$$\gamma_O = \gamma_{KO} + \Delta\gamma_O, \tag{6}$$

$$\psi_O = \psi_{KO} + \Delta\psi_O, \tag{7}$$

$$\gamma_H = \gamma_{KH} + \Delta\gamma_H, \tag{8}$$

$$\psi_H = \psi_{KH} + \Delta\psi_H. \tag{9}$$

From both the Laue equation at a Lorentz point used in Ewald–Von Laue's dynamical diffraction theory (Batterman & Cole, 1964; Colella, 1974; Zachariasen, 1967) and boundary conditions of the wavevector on the entrance surface, $\Delta\gamma_O$ and $\Delta\psi_O$ satisfy the following relation,

$$\xi\Delta\gamma_O + \eta\Delta\psi_O = (\chi_O^r/2)(1 + \cos\gamma_{KH}/\cos\gamma_{KO}), \tag{10}$$

where χ_O^r is the real part of the complex electric susceptibility. ξ and η are defined as

$$\xi = 2(\cos\gamma_{KO}\cos\beta + \sin\gamma_{KO}\cos\psi_{KO}\sin\beta) \times (\sin\gamma_{KO}\cos\beta - \cos\gamma_{KO}\cos\psi_{KO}\sin\beta), \tag{11}$$

$$\eta = 2(\cos\gamma_{KO}\cos\beta + \sin\gamma_{KO}\cos\psi_{KO}\sin\beta) \times \sin\gamma_{KO}\sin\psi_{KO}\sin\beta. \tag{12}$$

From the boundary conditions of the wavevector on the exit surface, $\Delta\gamma_H$ and $\Delta\psi_H$ are given by

$$\Delta\gamma_H = \left[-\cos\gamma_{KO}\cos(\psi_{KO} - \psi_{KH})\Delta\gamma_O + \sin\gamma_{KO}\sin(\psi_{KO} - \psi_{KH})\Delta\psi_O\right]/\cos\gamma_{KH}, \tag{13}$$

$$\Delta\psi_H = \left[-\cos\gamma_{KO}\sin(\psi_{KO} - \psi_{KH})\Delta\gamma_O - \sin\gamma_{KO}\cos(\psi_{KO} - \psi_{KH})\Delta\psi_O\right]/\sin\gamma_{KH}. \tag{14}$$

We cannot determine the angles of γ_O and ψ_O independently from (2) and (10). If we want to determine them independently, we need further geometrical relations between them.

For the RIDCM in which the incident polar angle γ_O is kept constant, the following two relations can be obtained,

$$\gamma_{KO} = \gamma = \text{constant}, \tag{15}$$

$$\Delta\gamma_O = 0. \tag{16}$$

By substituting (15) into (2),

$$\cos\psi_{KO} = [(H/2K) - \cos\gamma_{KO}\cos\beta]/\sin\gamma_{KO}\sin\beta, \tag{17}$$

is given. Substituting (16) into (10) yields

$$\Delta\psi_O = (\chi_O^r/2)(1 + \cos\gamma_{KH}/\cos\gamma_{KO})/\eta. \tag{18}$$

Therefore, for diffraction to occur, the crystal must be rotated about the normal **n** by $-\Delta\psi_O$.

4. Results and discussion

Before we investigate the real position of the exit X-ray from the RIDCM, we examine the coordinate transformation between O_1-XYZ and O_1-$X'Y'Z'$ (see Figs. 1 and 2). The position vector, (X', Y', Z') in O_1-$X'Y'Z'$, is represented by (X, Y, Z) in O_1-XYZ through

$$\begin{vmatrix} X' \\ Y' \\ Z' \end{vmatrix} = \mathbf{R} \begin{vmatrix} X \\ Y \\ Z \end{vmatrix}, \tag{19}$$

where the transformation matrix, **R**, is written as

$$\mathbf{R} = \begin{vmatrix} \sin\gamma_O\sin\psi_O\cos\beta/(1-\alpha^2)^{1/2} & (-\alpha\sin\gamma_O\cos\psi_O + \sin\beta)/(1-\alpha^2)^{1/2} & -\sin\gamma_O\cos\psi_O \\ (-\sin\gamma_O\cos\psi_O\cos\beta + \cos\gamma_O\sin\beta)/(1-\alpha^2)^{1/2} & -\alpha\sin\gamma_O\sin\psi_O/(1-\alpha^2)^{1/2} & -\sin\gamma_O\sin\psi_O \\ -\sin\gamma_O\sin\psi_O\sin\beta/(1-\alpha^2)^{1/2} & (-\alpha\cos\gamma_O + \cos\beta)/(1-\alpha^2)^{1/2} & -\cos\gamma_O \end{vmatrix} \tag{20}$$

Here, α is defined by

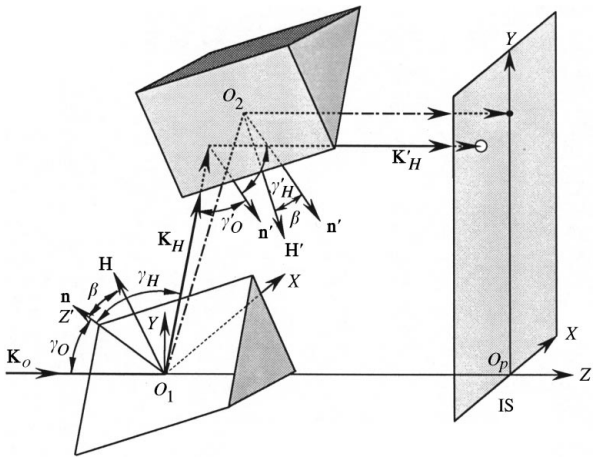

Figure 1
Schematic diagram of RIDCM. The O_1-XYZ coordinate system is fixed in an experimental hall. IS is the image screen perpendicular to the Z axis. O_1-$X'Y'Z'$ is fixed on the first crystal surface (see Fig. 2).

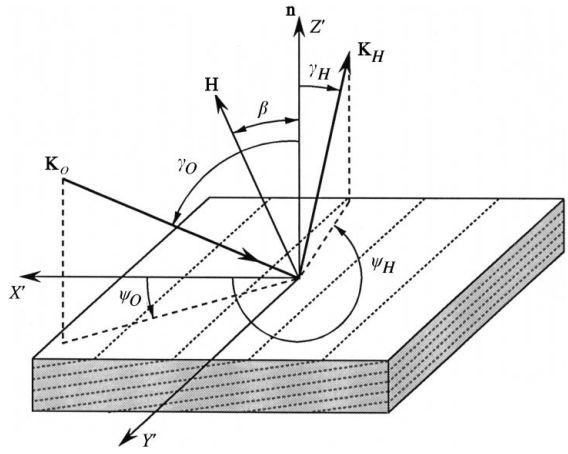

Figure 2
Schematic diagram of the scattering geometry on the first crystal surface.

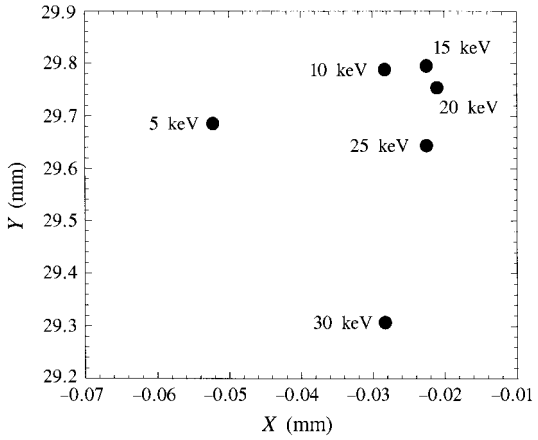

Figure 3
Position of exit X-rays from RIDCM at an X-ray energy 5, 10, 15, 20, 25 and 30 keV.

$$\alpha = \sin\gamma_O \cos\psi_O \sin\beta + \cos\gamma_O \cos\beta. \tag{21}$$

The second crystal surface through the point O_2, whose coordinate in O_1-XYZ is given by (1), is represented by

$$Z' = gr_{32} + gr_{33}/\tan 2\theta_B, \tag{22}$$

in O_1-$X'Y'Z'$, where r_{ij} is an element of the matrix $\mathbf{R}$. The diffracted X-ray from the first crystal, therefore, intersects the second crystal surface at the point

$$X' = Z' \sin\gamma_H \cos\psi_H/\cos\gamma_H, \tag{23}$$

$$Y' = Z' \sin\gamma_H \sin\psi_H/\cos\gamma_H, \tag{24}$$

in O_1-$X'Y'Z'$. The point shown in (22), (23) and (24) can be represented in O_1-XYZ as

$$\begin{vmatrix} X \\ Y \\ Z \end{vmatrix} = \mathbf{R}^{-1} \begin{vmatrix} X' \\ Y' \\ Z' \end{vmatrix}, \tag{25}$$

where matrix $\mathbf{R}^{-1}$ is the inverse of $\mathbf{R}$. Because the exit X-ray from the second crystal is parallel to the Z axis in O_1-XYZ, it intersects the image screen shown in Fig. 1 at the point (X, Y) given by (25).

The positions on the image screen of the exit X-ray from Si(111)-RIDCM, whose inclination angle (β) is 80°, at X-ray energies of 5, 10, 15, 20, 25 and 30 keV are shown in Fig. 3, where we assumed that the incident polar angle γ_O in (15) was 89° and that the nominal offset value g was 30.0 mm. The exit X-ray calculated in the kinematical theory intersects the image screen at the point (0, 30.0) mm. From Fig. 3 it is apparent that deviations of the exit positions for RIDCM are fairly great. The widths of deviation along X and Y directions are about 0.03 mm and 0.4 mm, respectively. Above and below an energy of about 20 keV, the deviations in RIDCM become larger. At about 20 keV the geometry of RIDCM is almost symmetric ($\gamma_O \simeq \gamma_H$). RIDCM takes on the grazing-incident geometry ($\gamma_O > \gamma_H$) at energies below 20 keV and the grazing-exit geometry ($\gamma_O < \gamma_H$) at higher energies. Because of the asymmetric geometry, the positions of the exit X-rays from RIDCM vary over a wide range.

We now discuss how to suppress this deviation of exit X-ray position. The reciprocal lattice vector $\mathbf{H}$ does not lie in the plane of incidence containing both the incident wavevector $\mathbf{K}_O$ and the diffracted one $\mathbf{K}_H$ because of refraction. Therefore, when we put $\mathbf{H}$ in the Y-Z plane, we cannot obtain the exit X-ray at $X = 0$. We introduce the scattering vector $\mathbf{H}_S$, defined as

$$\mathbf{H}_S = \mathbf{K}_O - \mathbf{K}_H. \tag{26}$$

From the boundary conditions of the wave vectors on both the incident and exit crystal surfaces, we can obtain the important result that $\mathbf{H}_S$ always lies in the plane spanned with $\mathbf{H}$ and $\mathbf{n}$ (Colella, 1974). We define β' to be the angle between $\mathbf{H}_S$ and $\mathbf{n}$ and express it as

$$\beta' = \beta + \Delta\beta. \tag{27}$$

$\Delta\beta$ can be approximately written from the boundary conditions of the wave vectors as

$$\Delta\beta = -(K/H)\zeta \sin\beta, \tag{28}$$

where

$$\zeta = -\sin\gamma_{KO}\Delta\gamma_O - \sin\gamma_{KH}\Delta\gamma_H. \tag{29}$$

We find from these equations that $\Delta\beta$ depends on both the X-ray energy and the geometry of the monochromator.

It is required from (26) that we always put $\mathbf{H}_S$ in the Y-Z plane to keep the exit X-ray in the Y-Z plane. The actual scattering angle of the X-ray diffracted by the crystal is different from $2\theta_B$ as calculated by the kinematical diffraction theory, and is given by

$$\begin{aligned}\cos 2\theta = &-\sin\gamma_O \cos\psi_O \sin\gamma_H \cos\psi_H \\ &-\sin\gamma_O \sin\psi_O \sin\gamma_H \sin\psi_H - \cos\gamma_O \cos\gamma_H.\end{aligned} \tag{30}$$

We finally translate the second crystal from O_1 to O_2, where the translation vector $\overline{O_1O_2}$ is given by (1) but we replace $2\theta_B$ in (1) with 2θ in (30). Then, we can fix the exit position at the point $(X, Y) = (0, g)$ on the image screen shown in Fig. 1.

References

Batterman, B. W. & Cole, H. (1964). *Rev. Mod. Phys.* **36**, 681–717.
Blasdell, R. C., Macrander, A. T. & Lee, W. K. (1994). *Nucl. Instrum. Methods*, A**347**, 327–330.
Colella, R. (1974). *Acta Cryst.* A**30**, 413–422.
Hrdy, V. (1992). *Rev. Sci. Instrum.* **63**, 459–460.
Khounsary, A. M. (1992). *Rev. Sci. Instrum.* **63**, 461–464.
Lee, W. K., Macrander, A. T., Mills, D. M., Rogers, C. S., Smither, R. K. & Berman, L. E. (1992). *Nucl. Instrum. Methods*, A**320**, 381–387.
Lee, W. K. & Mills, D. M. (1994). *Nucl. Instrum. Methods*, A**347**, 618–626.
Macrander, A. T., Lee, W. K., Smither, R. K., Mills, D. M., Rogers, C. S. & Khounsary, A. M. (1992). *Nucl. Instrum. Methods*, A**319**, 188–196.
Uruga, T., Kimura, H., Kohmura, Y., Kuroda, M., Nagasawa, H., Ohtomo, K., Yamaoka, H., Ishikawa, T., Ueki, T., Iwasaki, H., Hashimoto, S., Kashihara, Y. & Okui, K. (1995). *Rev. Sci. Instrum.* **66**, 2254–2256.
Zachariasen, W. H. (1967). *Theory of X-ray Diffraction in Crystals*. New York: Dover.